βII-spectrin promotes mouse brain connectivity through stabilizing axonal plasma membranes and enabling axonal organelle transport

Damaris N. Lorenzo[a,1], Alexandra Badea[b], Ruobo Zhou[c,d,e], Peter J. Mohler[f], Xiaowei Zhuang[c,d,e], and Vann Bennett[g,1]

[a]Department of Cell Biology and Physiology, The University of North Carolina at Chapel Hill, Chapel Hill, NC 27599; [b]Department of Radiology, Duke University, Durham, NC 27708; [c]Howard Hughes Medical Institute, Harvard University, Cambridge, MA 02138; [d]Department of Chemistry and Chemical Biology, Harvard University, Cambridge, MA 02138; [e]Department of Physics, Harvard University, Cambridge, MA 02138; [f]Department of Physiology and Cell Biology, The Ohio State University Wexner Medical Center, Columbus, OH 43210; and [g]Department of Biochemistry, Duke University, Durham, NC 27710

Contributed by Vann Bennett, May 14, 2019 (sent for review December 6, 2018; reviewed by Nobutaka Hirokawa, Erika L. F. Holzbaur, and Subhojit Roy)

βII-spectrin is the generally expressed member of the β-spectrin family of elongated polypeptides that form micrometer-scale networks associated with plasma membranes. We addressed in vivo functions of βII-spectrin in neurons by knockout of βII-spectrin in mouse neural progenitors. βII-spectrin deficiency caused severe defects in long-range axonal connectivity and axonal degeneration. βII-spectrin–null neurons exhibited reduced axon growth, loss of actin–spectrin-based periodic membrane skeleton, and impaired bidirectional axonal transport of synaptic cargo. We found that βII-spectrin associates with KIF3A, KIF5B, KIF1A, and dynactin, implicating spectrin in the coupling of motors and synaptic cargo. βII-spectrin required phosphoinositide lipid binding to promote axonal transport and restore axon growth. Knockout of ankyrin-B (AnkB), a βII-spectrin partner, primarily impaired retrograde organelle transport, while double knockout of βII-spectrin and AnkB nearly eliminated transport. Thus, βII-spectrin promotes both axon growth and axon stability through establishing the actin–spectrin-based membrane-associated periodic skeleton as well as enabling axonal transport of synaptic cargo.

neuronal cytoskeleton | axonal transport | axonal growth | spectrin | STORM

Spectrins are elongated proteins that form extended plasma membrane-associated networks cross-linked by short actin filaments and cooperate with ankyrins to coordinate functionally related proteins within plasma membrane domains (1, 2). A spectrin–actin network was first discovered in mammalian erythrocytes, which contain only a plasma membrane, but spectrin assemblies are also associated with specialized plasma membranes in epithelial cells, neurons, cardiomyocytes, and skeletal muscle (1, 2). Plasma membrane-associated spectrin–actin networks in erythrocytes form a 2D polygonal structure, as first observed by electron microscopy (3). Superresolution light microscopy has revealed similar structures in neuronal cell bodies and parts of the dendrites, as well as a quasi-1D periodic structure in axons and dendrites (4, 5). These structures are based on the principle of 190-nm spectrin tetramers cross-linked by multivalent short actin filaments that are capped by actin-capping proteins such as adducin (1, 2, 6) (see Fig. 3*D*). The flexible nature of spectrin results in either polygonal networks, where spectrin tetramers connect individual short actin filaments at the nodes of the polygons (3, 7), or ring-like structures of aligned actin filaments that wrap the circumference of axons and parts of the dendrites evenly spaced by spectrin tetramers (4, 5). Both configurations confer mechanical stability on a cellular scale: Deficiency of spectrin results in fragility of erythrocytes and fragmentation of axons (8, 9). Noteworthily, other actin networks coexist with actin rings and polygons in neurons (10).

Spectrins and ankyrins also have been implicated in microtubule-dependent transport of intracellular organelles (11–15). The dynein/dynactin motor complex drives neuronal microtrubule-based transport in the retrograde direction, while a diverse group of kinesin motors move cargo anterogradely (16). Unlike dynein, kinesins belong to a superfamily of proteins (KIFs) that include over 40 genes, although not all members are involved in neuronal transport (16). Both dynein and kinesins are involved in neuronal disease pathogenesis (16). Initial evidence of spectrins' involvement in transport emerged from the observation that a pair of high-molecular-weight polypeptides, termed fodrin, comigrated with multiple classes of axonal organelles following metabolic pulse labeling of axonal cargo in the optic nerve (11). Subsequent identification of these polypeptides as α- and β-spectrin led to a focus on their plasma membrane roles (17). Nevertheless, other reports have supported the functional connections of both spectrin and ankyrin with organelle trafficking. For example, αII-spectrin associates with the kinesin motor KIF3 and with axonal organelles in rats, and it moves with similar velocities as KIF3 in pulse-chase experiments (12). Moreover, the dynactin complex binds spectrin through Arp1 (18) and ankyrin-B (AnkB) through p62/dynactin-4 (19). Expression of *Drosophila* β-spectrin bearing human βIII-spectrin mutations causing spinocerebellar ataxia type 5 (SCA5) results in impaired neuronal organelle transport in flies (13). AnkB associates with endolysosomal organelles through PI3P lipids and is required for their axonal transport (14) and for polarized recycling of α5/β1 integrin dimers in migrating fibroblasts (15).

These divergent functions of spectrins and ankyrins raise the question of whether specialized family members and isoforms are dedicated to either plasma membrane structure or organelle transport, or if the same polypeptides perform both roles. In the

Significance

Establishment and maintenance of long axonal projections are essential for brain development and function of the nervous system. Plasma membrane-associated structural proteins promote axon stability and efficient organelle transport, which is thought to be critical in supporting axonal elongation, while both activities are essential for long-term survival of neurons. This study demonstrates that βII-spectrin in axons enables organelle bidirectional transport in addition to its previously established role in forming a periodic membrane-associated actin–spectrin skeleton. βII-spectrin thus promotes both axon stability and axon growth through biochemically distinct functions.

Author contributions: D.N.L. and V.B. designed research; D.N.L., A.B., and R.Z. performed research; D.N.L., A.B., R.Z., P.J.M., and X.Z. contributed new reagents/analytic tools; D.N.L., A.B., R.Z., and X.Z. analyzed data; and D.N.L. and V.B. wrote the paper.

Reviewers: N.H., University of Tokyo; E.L.F.H., University of Pennsylvania; and S.R., University of Wisconsin–Madison.

The authors declare no conflict of interest.

See Commentary on page 15324.

[1]To whom correspondence may be addressed. Email: damaris_lorenzo@med.unc.edu or benne012@mc.duke.edu.

This article contains supporting information online at www.pnas.org/lookup/suppl/doi:10.1073/pnas.1820649116/-/DCSupplemental.

Published online June 17, 2019.

case of ankyrins, AnkB (encoded by the *ANK2* gene) associates with intracellular organelles and this activity depends upon a single exon that diverged from ankyrin-G (AnkG, encoded by the *ANK3* gene) early in vertebrate evolution (20). Four vertebrate β-spectrins share ankyrin-binding activity, and three of them exhibit tissue-specific expression. βI-spectrin is primarily found in erythrocytes, striated muscle, and a subset of neurons. βIII-spectrin is expressed at highest levels in the cerebellum, where it is enriched in dendrites of Purkinje neurons, but it is also expressed in other areas of the brain (21). βIV-spectrin similarly exhibits cell-type-specific expression in neurons and pancreatic β-cells (1, 2, 22). Consistent with these restricted expression patterns, mice and humans lacking these β-spectrins are viable, although with serious phenotypes, including severe anemia for βI-spectrin (23), cerebellar ataxia for βIII-spectrin (24), and abnormal neural development for βIV-spectrin (25). βII-spectrin, in contrast to other members of the β-spectrin family, is expressed in most cell types (although not in mature erythrocytes), and whole-body βII-spectrin knockout (KO) mice die by embryonic day (E)12 (26).

Here, we find that KO of βII-spectrin targeted to neuronal progenitors results in major loss of long-range axonal connectivity as well as axonal degeneration. βII-spectrin–deficient neurons have reduced axonal growth in vitro and exhibit loss of periodic actin rings. However, loss of βII-spectrin also markedly impairs bidirectional transport of synaptic organelles in axons. We determined that βII-spectrin associates with the dynein/dynactin motor complex, and several kinesins. Our results suggest that assembly of the periodic actin–spectrin-based membrane skeleton is not required to enable the intracellular transport machinery. Finally, we establish that the deficits in transport caused by loss of βII-spectrin are independent of its interaction with AnkB. Together these findings demonstrate that βII-spectrin multitasks in vivo as a critical structural component of axonal plasma membranes as well as an enabler of axonal organelle transport.

Results

Loss of Central Nervous System βII-Spectrin Causes Loss of Brain Connectivity. To determine functional roles of βII-spectrin in neurons in vivo, we crossed mice homozygous for the βII-spectrin floxed allele ($\beta IISp^{flox/flox}$) developed by Rasband and coworkers (27) with Nestin-Cre mice, which express Cre-recombinase in neural progenitor cells. We confirmed over 90% reduction of brain βII-spectrin levels in $\beta IISp^{flox/flox}$/Nestin-Cre (βII-SpKO) mice by immunofluorescence staining (Fig. 1*A*) and by immunoblot analysis of total brain homogenates and culture neurons (*SI Appendix*, Fig. S1*A*). The residual βII-spectrin signal in βII-SpKO mice is likely contributed by brain endothelial cells and a small population of neurons that escaped Cre recombination. Depletion of neural βII-spectrin slightly reduced levels of αII-spectrin, its obligatory partner, and 440-kDa and 220-kDa isoforms of AnkB (*SI Appendix*, Fig. S1 *B* and *C*). In contrast, we detected no changes in the expression of βIII-spectrin, AnkG, or βIV-spectrin∑1 but significant elevations in βIV-spectrin ∑6 isoform and ankyrin-R (AnkR) at postnatal day (PND)25 (*SI Appendix*, Fig. S1 *B* and *C*). Together, these data suggest that other cytoskeletal proteins do not compensate for the embryonic loss of βII-spectrin, except for βIV-spectrin ∑6, which is predominantly expressed in the postnatal brain and localized to axon initial segments (AIS) (28), and AnkR, which is expressed in a subset of forebrain and cerebellar neurons (29, 30).

Conditional βIISp-KO mice were born at expected ratios but were smaller than $\beta IISp^{flox/flox}$ (βIISp-WT) littermate controls (Fig. 1*B*), with motor coordination deficits and multiple seizures (*SI Appendix*, Fig. S2*B*). βIISp-KO mice experienced early postnatal lethality between PND15 and PND45 (*SI Appendix*, Fig. S2*A*), as previously reported (27). Histological characterization of PND0 and PND6 βII-SpKO brains revealed either complete absence or significant reduction of long axonal bundles connecting cerebral hemispheres, including the corpus callosum (CC) (Fig. 1*A* and, *SI Appendix*, Fig. S2*C*). We next implemented an MRI- and diffusion tensor imaging (DTI)-based protocol with compressed sensing, which delineates white matter structures in the brain and allows 3D reconstruction of axonal tracts (31). Fractional anisotropy (FA) maps derived from DTI images from βII-SpKO PND25 brains show loss or complete absence of long axonal projections, including those in the CC (Fig. 1 *C* and *D*, yellow inset). Analysis of 3D-reconstructed fibers revealed that βII-SpKO brains have a major reduction in the average length of axons (Fig. 1*G*) and in FA values, which is indicative of loss of axonal integrity (Fig. 1*H*). βII-spectrin deficiency thus leads to widespread deficits in axonal length and long axon tracts.

Loss of βII-Spectrin Results in Larger-Caliber Axons and Axonal Degeneration. To determine if loss of βII-spectrin compromises axon survival, we examined the ultrastructural organization of

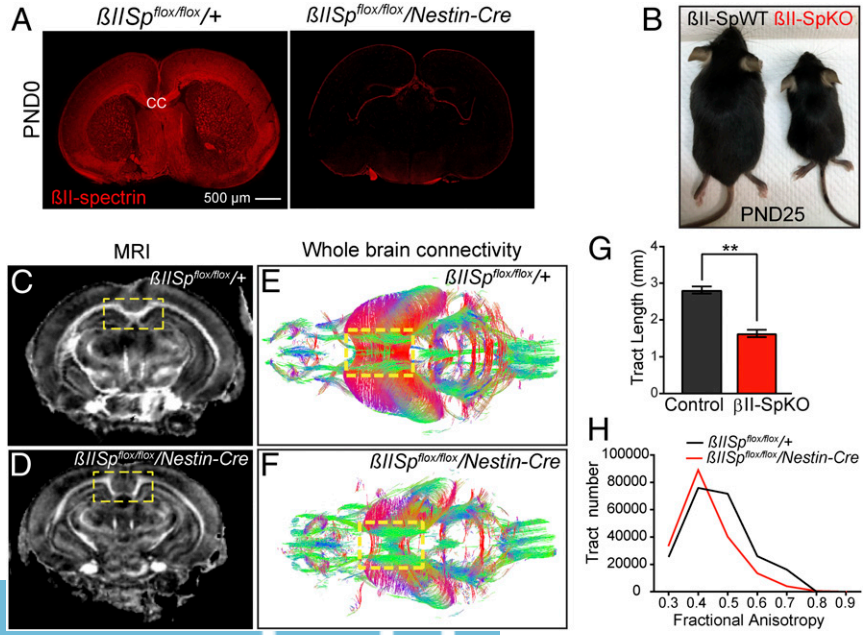

Fig. 1. Brain βII-spectrin is required for axonal integrity and long-range axonal connectivity. (*A*) $\beta IISp^{flox/flox}$/+ and $\beta IISp^{flox/flox}$/Nestin-Cre PND0 brains stained for βII-spectrin. (Scale bar, 500 μm.) (*B*) PND25 $\beta IISp^{flox/flox}$/+ (βII-SpWT) and $\beta IISp^{flox/flox}$/Nestin-Cre (βII-SpKO) mice. (*C* and *D*) FA maps of $\beta IISp^{flox/flox}$/+ (*F*) and $\beta IISp^{flox/flox}$/Nestin-Cre (*G*) PND21 brains derived from DTI. (*E* and *F*) Three-dimensional images of white matter tracts from $\beta IISp^{flox/flox}$/+ (*E*) and $\beta IISp^{flox/flox}$/Nestin-Cre (*F*) mice colored by FA values. The yellow box indicates the position of the CC, which is absent in $\beta IISp^{flox/flox}$/Nestin-Cre mice. (*G*) Analysis of white matter track length in $\beta IISp^{flox/flox}$/+ ($n = 6$) and $\beta IISp^{flox/flox}$/Nestin-Cre ($n = 7$) brains. Data represent mean ± SEM. Student's *t* test, $^{**}P < 0.01$. (*H*) FA distribution of white matter tracks in $\beta IISp^{flox/flox}$/+ ($n = 6$) and $\beta IISp^{flox/flox}$/Nestin-Cre ($n = 7$) brains.

long-range axons, using transmission electron microscopy (TEM) of cross-section of the CC. PND25 βII-SpKO brains showed a significant increase in the diameter of myelinated axons relative to controls (Fig. 2 *A–E* and *SI Appendix*, Fig. S3 *B* and *C*). Furthermore, brains from βII-SpKO mice showed signs of axonal degeneration, including myelin sheath decompaction and vacuolization (Fig. 2*D*, red asterisks) and dense material in the cytosol, likely reflecting breakdown of cytoskeletal elements (Fig. 2*D*, blue asterisk), and the appearance of neuroinflammatory microglia (Fig. 2*B* and *SI Appendix*, Fig. S3*A*, red arrowhead). The g-ratio (ratio of diameters of inner axon and outer fiber) also increased, indicating thinning of the myelin sheet (Fig. 2*F*). These changes in myelin organization were predominantly found in large-diameter axons (Fig. 2*F*, red circle). Loss of myelin was not associated with a decrease in myelin basic protein expression (*SI Appendix*, Fig. S1 *B* and *C*). These observations suggest that βII-spectrin is required for maintenance of myelinated axons, which form and subsequently undergo degeneration. Interestingly, loss of αII-spectrin in myelinated peripheral sensory neurons in mice also resulted in preferential loss of larger-diameter axons as the mice aged, which was attributed to a protective role of αII-spectrin in larger-diameter axons (32). Neurons lacking α-adducin, which is also periodically incorporated into the periodic axonal structure (4), form an axonal actin periodic structure but develop axons with slightly enlarged actin rings and calibers (33).

βII-Spectrin Promotes Axonal Growth of Cultured Neurons. To investigate the contribution of βII-spectrin to axon growth, we evaluated cortical neurons cultured from wild-type (WT) and βII-SpKO E15.5 embryos. Loss of βII-spectrin did not affect axonal specification, including formation of the AIS. We detected normal clustering of AnkG at the AIS (*SI Appendix*, Fig. S4 *A*, asterisk and *SI Appendix*, Fig. *C*). The length of the AIS in both day in vitro (DIV)11 βII-SpKO cultured neurons (*SI Appendix*, Fig. S4 *A* and *B*) and in cortical slices of PND6 βII-SpKO brains (*SI Appendix*, Fig. S4 *C* and *D*) was also normal. Similarly, loss of βII-spectrin does not affect the normal polarized distribution of axonal versus dendritic proteins in neurons, as indicated by the normal localization of transferrin receptor (TfR-mCherry) and the trans-Golgi network protein 38 (TGN38-YFP) in dendrites of DIV11 βII-SpKO neurons (*SI Appendix*, Fig. S5 *A* and *B*), where they preferentially localized normally. Consistent with the reduction in axonal length observed in βII-SpKO brains, loss of βII-spectrin caused significant reduction in the length of the axons in cortical (Fig. 3 *A–C*) and hippocampal (*SI Appendix*, Fig. S6) cultured neurons. Rescue with mScarlet-tagged βII-spectrin resulted in restoration of axon length to WT values (Fig. 3 *B* and *C*). βII-spectrin, thus, is not required for initial stages of axonal formation and neuronal polarization but rather promotes the growth and maintenance of axonal processes once they are established.

The Periodic Actin Ring Structure in Axons Is Disrupted in βII-Spectrin–Deficient Neurons. Loss of βII-spectrin in cultured neurons using acute short hairpin RNA knockdown disrupts the periodic actin arrangement (4, 5). We conducted 3D stochastic optical reconstruction microscopy (STORM) imaging (34, 35) of hippocampal neuronal cultures derived from E15.5 mice lacking neuronal βII-spectrin through embryonic development. Loss of βII-spectrin largely disrupted the 190-nm-based periodic distribution of actin and adducin in axons of DIV14 neurons (Fig. 4 *A–E*), with a higher level of residual periodic structures observed in neurons at DIV20 (Fig. 4 *F–J*), suggesting the possibility of a gradual, partial compensation. In general, the level of residual periodic structures in βII-spectrin–depleted neurons was higher in axon regions proximal to the soma. Loss of βII-spectrin also substantially disrupted the periodic structures in dendrites (*SI Appendix*, Fig. S7 *A–E*). These results confirm that βII-spectrin is important for the formation of the periodic membrane skeleton structure. The periodic membrane skeletal network likely confers stability to axons, and loss of this structure likely contributes to the axonal degeneration noted in βII-spectrin–deficient brains (Fig. 2).

Loss of βII-Spectrin Does Not Directly Affect Microtubule Dynamics. Recent studies using actin-destabilizing drugs suggest that cortical actin plays microtubule-maintaining roles in axons, and that the abundance of axonal actin rings directly correlates with axonal microtubule organization (36). To determine whether loss of βII-spectrin and the resulting disruption of the actin–spectrin periodic network impairs microtubule dynamics, we followed the localization of the microtubule plus end-associated protein EB3-tdTomato in live neurons. Movies from transfected DIV5 cortical neurons and kymograph analysis show a similar average number of EB3-tdT comets (*SI Appendix*, Fig. S8*A*, asterisks) moving toward microtubule growing ends in control and βII-SpKO cells (*SI Appendix*, Fig. S8*B*). Similarly, we found that βII-SpKO axonal microtubules have normal velocity and run length of EB3-tdT comets (*SI Appendix*, Fig. S8 *C* and *D*). TEM cross-sections of non-degenerating CC axons from control and βII-SpKO mouse brains where we were able to detect microtubule structures did not reveal clear differences in microtubule arrangement or numbers between phenotypes, although reliable quantitative analysis was not possible because the microtubule bundles were not always unequivocally distinguishable in our samples (*SI Appendix*, Fig. S8*E*). These data

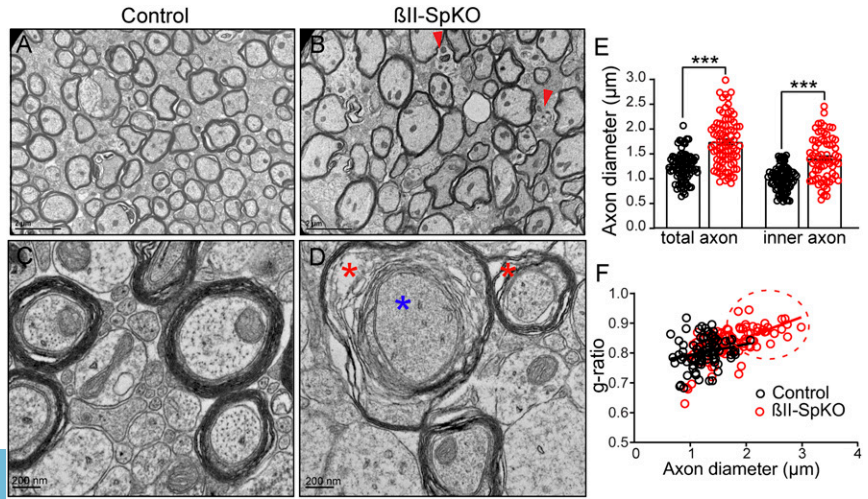

Fig. 2. βII-spectrin maintains the caliber and integrity of myelinated CC axons. (*A* and *B*) TEM images of cross-sections through the CC from *βIISp*$^{flox/flox}$/+ (*A*, control) and *βIISp*$^{flox/flox}$/Nestin-Cre (*B*, βII-SpKO) PND25 mice (n = 3 mice). Red arrowheads indicate inflammatory microglia. (Scale bars, 2 μm.) (*C* and *D*) Higher-magnification images of CC axons from control (*C*) and βII-SpKO (*D*) mice. Asterisks indicate degenerating axons with decompaction of the myelin sheath and vacuolization (red asterisks) and debris (blue asterisk). (Scale bars, 200 nm.) (*E*) Comparison of myelinated axon diameter from control (n = 85) and βII-SpKO (n = 84) CC axons. Data represent mean ± SEM. Student's t test, ***$P < 0.001$. (*F*) g-ratio versus axon diameter from CC of PND25 control and βII-SpKO mice. Red dotted circle area represents a population of βII-SpKO large-diameter axons with decreased myelin content that is absent in control brains.

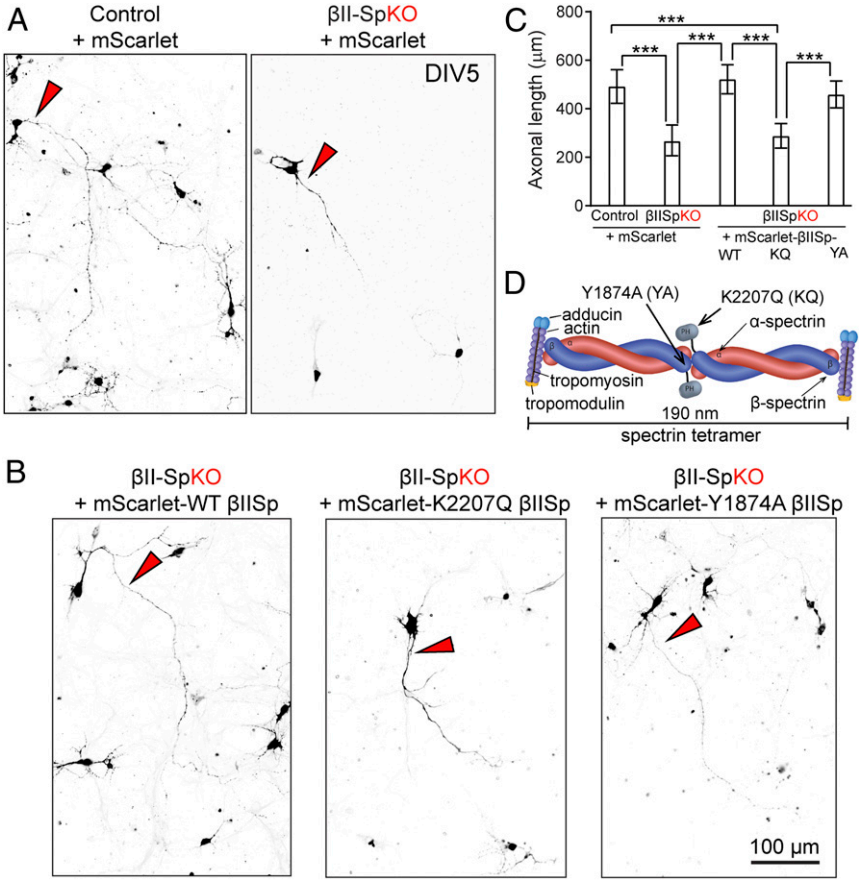

Fig. 3. βII-spectrin is required for axonal elongation of cultured neurons. (*A*) DIV5 control or βII-SpKO cortical neurons transfected at DIV0 with pmScarlet. (*B*) DIV5 βII-SpKO cortical neurons transfected at DIV0 with pmScarlet-tagged WT βII-Spectrin or indicated mutants. Red arrowheads in *A* and *B* indicate axons. (Scale bar, 100 μm.) (*C*) Axonal length in control ($n = 12$), βII-SpKO ($n = 8$), and βII-SpKO neurons rescued with WT-βIISp ($n = 7$), K2207Q-βIISp ($n = 7$), and Y1974A-βIISp ($n = 7$) constructs. Data represent mean ± SEM. One-way ANOVA with Dunnett's multiple comparisons test, ***$P < 0.001$. (*D*) Schematic of spectrin tetramer organization in axons comprising dimers of α-spectrin and β-spectrin that cross-link short actin filaments capped by adducin and tropomodulin and determine their periodic distribution every 200 nm in axons. The Y1874A and K2207Q mutations respectively abrogate binding to ankyrin or PIP lipids.

suggest that loss of βII-spectrin does not directly alter microtubule dynamics and may not affect microtubule stability. However, other downstream progressive effects caused by loss of βII-spectrin, such as axonal degeneration (Fig. 2*B* and *SI Appendix*, Fig. S3, red arrowhead, and Fig. 2*D*, red asterisks), likely disrupt microtubule tracks (Fig. 2*D*, blue asterisk).

βII-Spectrin Promotes Bidirectional Multiorganelle Transport in Axons. Neurons rely on the transport of organelles to grow and maintain dendrites and axons (37, 38). Spectrins have been suggested to function as cargo adaptors in axonal transport, as discussed above. Therefore, we hypothesized that the reduced axonal length phenotypes observed in βII-SpKO brains and cultured neurons are associated with impaired axonal cargo motility. We tested this hypothesis by tracking the dynamics of yellow fluorescent protein (YFP)-tagged synaptophysin (a synaptic vesicle marker) in hippocampal neuron cultures from control and βII-SpKO brains using time-lapse video microscopy. Loss of βII-spectrin in neurons impaired bidirectional synaptic vesicle transport. We detected significant reduction in the percentage of motile cargo and overall flux in βII-SpKO axons (Fig. 5 *A*–*C*). Similarly, we observed differences in both velocity and displacement of motile synaptic vesicles (Fig. 5 *D* and *E*), with the most severe effects observed on anterograde motion. Loss of βII-spectrin also impaired the bidirectional flux of LAMP1-green fluorescent protein–positive endosome/lysosome vesicles (*SI Appendix*, Fig. S9 *A*, *D*, and *E*) and caused significant deficits in their run length and retrograde velocity (*SI Appendix*, Fig. S9 *B* and *C*). The differences in the motility of synaptic versus endolysosomal cargo in βII-SpKO axons likely reflect known intrinsic bias in transport direction for each of these cargos and potential selective effects of loss of βII-spectrin on particular anterograde motors required for their motion. Nonetheless, deficits in transport of both synaptic cargo and lysosomes were rescued by expression of mScarlet-tagged WT βII-spectrin (Fig. 5 *A*–*E* and *SI Appendix*, Fig. S9).

To evaluate whether βII-spectrin functions as a motor effector, we first evaluated its association with both anterograde and retrograde motor proteins via immunoprecipitation from whole-brain protein homogenates. We found that, similar to αII-spectrin (12), βII-spectrin associates with KIF3A (Fig. 6*D*). In addition, βII-spectrin also coimmunoprecipitates with KIF1A and KIF5B as well as the $p150^{Glued}$ subunit of the dynactin complex (Fig. 6*D*). Second, we confirmed that βII-spectrin associates with intracellular membranes and found strong enrichment of βII-spectrin in cellular fractions containing synaptic vesicles isolated through subcellular fractionation of crude total brain homogenates (Fig. 6*A*, membrane). Strikingly, loss of βII-spectrin in βII-SpKO brains reduced the association of KIF1A, KIF5B, KIF3A, and the $p150^{Glued}$ subunit of the dynactin complex with intracellular membranes (Fig. 6 *A* and *B*), while the total expression of these motors in brain postnuclear supernatant fractions was unchanged (Fig. 6*C*). Taken together, these data indicate that βII-spectrin associates with both motor protein and

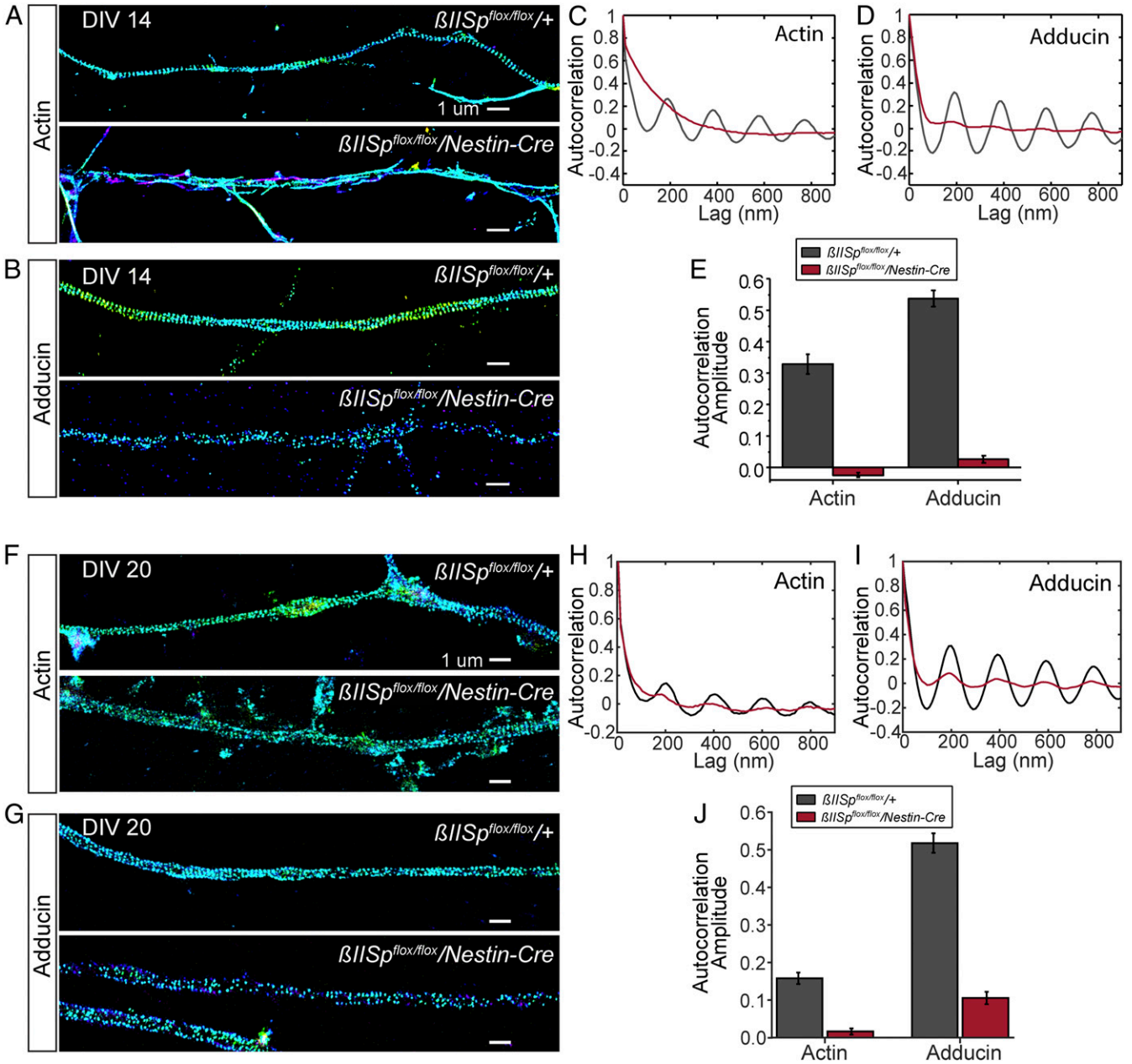

Fig. 4. βII-spectrin is important for the assembly of the actin–spectrin-based periodic membrane skeleton structure in axons. (*A* and *B*) Three-dimensional STORM images of actin (*A*) and adducin (*B*) in axons of DIV14 control and βII-SpKO neurons. (Scale bars, 1 μm.) (*C* and *D*) Average autocorrelation functions of actin (*C*) and adducin (*D*) calculated from multiple, randomly selected axonal regions. Actin: $n = 96$ for $\beta IISp^{flox/flox}/+$ samples and ($n = 128$) for $\beta IISp^{flox/flox}$/Nestin-Cre samples. Adducin: $n = 95$ for $\beta IISp^{flox/flox}/+$ samples and ($n = 148$) for $\beta IISp^{flox/flox}$/Nestin-Cre samples. (*E*) Average autocorrelation amplitudes corresponding to actin (*C*) and adducin (*D*) periodicity functions in axons. (*F* and *G*) Three-dimensional STORM images of actin (*F*) and adducin (*G*) in axons of DIV20 control and βII-SpKO neurons. (Scale bars, 1 μm.) (*H* and *I*) Average autocorrelation functions of actin (*H*) and adducin (*I*) calculated from multiple, randomly selected axonal regions. Actin: $n = 167$ for $\beta IISp^{flox/flox}/+$ samples and $n = 199$ for $\beta IISp^{flox/flox}$/Nestin-Cre samples. Adducin: $n = 130$ for $\beta IISp^{flox/flox}/+$ samples and $n = 130$ for $\beta IISp^{flox/flox}$/Nestin-Cre samples. (*J*) Average autocorrelation amplitudes corresponding to actin (*H*) and adducin (*I*) periodicity functions in axons. Data represent mean ± SEM. The lower autocorrelation amplitude observed for actin in DIV20 versus DIV14 control neurons is likely because a stronger fixative (glutaraldehyde), which better preserve actin filaments, was used for DIV14 neurons, whereas DIV20 neurons were fixed with paraformaldehyde.

cargoes and may play a prominent role in coupling motor proteins to membranes.

βII-Spectrin Promotes Normal Organelle Axonal Transport in the Absence of Periodic Actin Rings. Loss of βII-spectrin largely disrupts the organization of periodic actin rings in axons in neurons imaged at DIV14 (Fig. 4) and results in impaired axonal transport in DIV7 neurons (Fig. 5 and *SI Appendix*, Fig. S9). Loss of βII-spectrin also causes significant reduction in the length of the axons in cultured neurons, which is apparent as early as DIV5 (Fig. 3 *B* and *C*). Axons lacking βII-spectrin are prone to deteriorate, as evidenced by signs of degeneration observed in electron microscopy (EM) sections of callosal axons from PND25 βII-SpKO brains (Fig. 2 *B* and *D* and *SI Appendix*, Fig. S3). The onset of axonal degeneration in βII-spectrin KO neurons likely happens much earlier, and as noted above, and it is

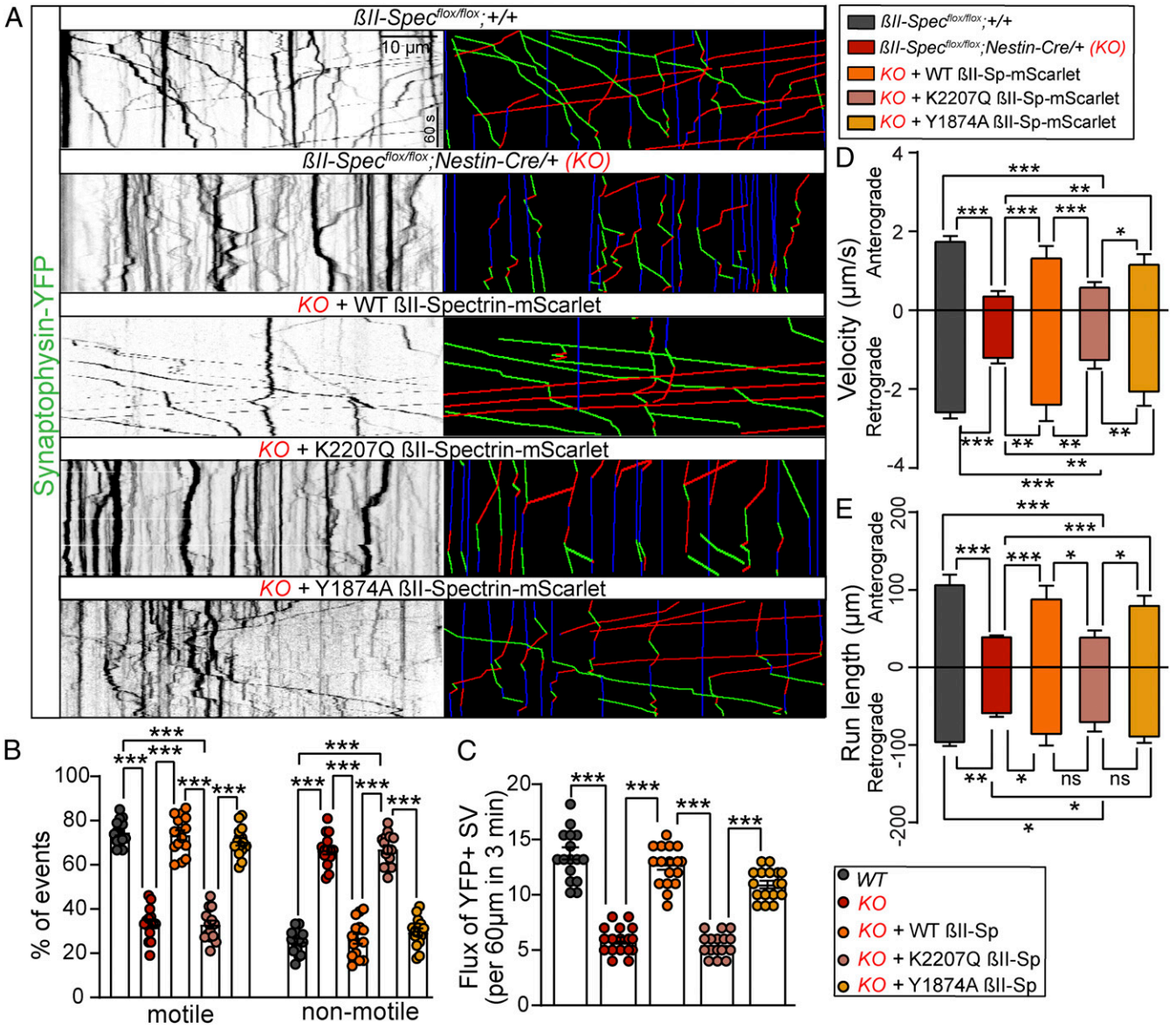

Fig. 5. βII-spectrin promotes bidirectional axonal transport. (*A*) Kymographs showing motility of YFP-tagged synaptophysin-positive synaptic vesicles in axons of DIV7 neurons from the indicated genotypes. Trajectories are shown in green for anterograde, red for retrograde, and blue for static vesicles. (Scale bar, 10 µm and 60 s.) (*B–E*) Relative number of motile and nonmotile synaptic vesicles (*B*), quantification of flux (*C*), anterograde and retrograde velocity (*D*), and run length (*E*) of synaptic vesicles for each genotype and rescue in $\beta IISp^{flox/flox}$/+ ($n = 15$), $\beta IISp^{flox/flox}$/Nestin-Cre (KO) ($n = 17$), KO + WT βII-mScarlet ($n = 12$), KO + K2207Q βII-mScarlet ($n = 11$), and KO + Y1874A βII-mScarlet ($n = 10$) axons of DIV7 neurons. Data represent mean ± SEM. One-way ANOVA with Dunnett's multiple comparisons test, $***P < 0.001$, $**P < 0.01$, $*P < 0.05$. ns, not significant.

expected to cause disruptions in the transport machinery. Thus, an important question is whether the transport defects observed in βII-spectrin KO maturing neurons may be indirectly caused by the deficits in axonal outgrowth. To address this question, we tracked the dynamics of YFP-tagged synaptophysin in DIV2 control and βII-SpKO cortical neuronal cultures, when differences in axonal length are not very pronounced (Fig. 7 *A, B*, and *E*). Like in DIV7 βII-spectrin KO neurons, bidirectional synaptic vesicle transport is already impaired in DIV2 axons lacking βII-spectrin, as reflected by the significant reduction in number of motile vesicles and overall flux (Fig. 7 *D, G*, and *H*). These results indicate that the deficits in axonal transport caused by loss βII-spectrin precede overt deficits in axonal outgrowth and degeneration.

As shown above, disruption of the axonal actin–spectrin periodic structure caused by loss of βII-spectrin does not directly affect microtubule dynamics. However, it is not clear whether the presence of the axonal actin–spectrin periodic structure is a prerequisite for the enablement of normal axonal transport. To begin to answer this question, we took advantage of the proximal-to-distal axon, progressive formation of the actin–spectrin periodic structure (39) to correlate organelle transport with actin rings along the axon. As previously reported (39), we detected an actin–spectrin periodic structure in the proximal (Fig. 7*A*, A1) but not in the distal (Fig. 7*A*, A2) axonal region of DIV2 control neurons, which is consistent with the rate of propagation of the periodic structure along the axons (39). As expected, actin–spectrin periodicity was lacking along the length of DIV2 βII-spectrin KO axons (Fig. 7*B*, B1 and B2). We imaged synaptic vesicle dynamics in both the proximal and the distal axon regions of control neurons and noticed no difference in their motilities or flux between those regions (Fig. 7 *C, G*, and

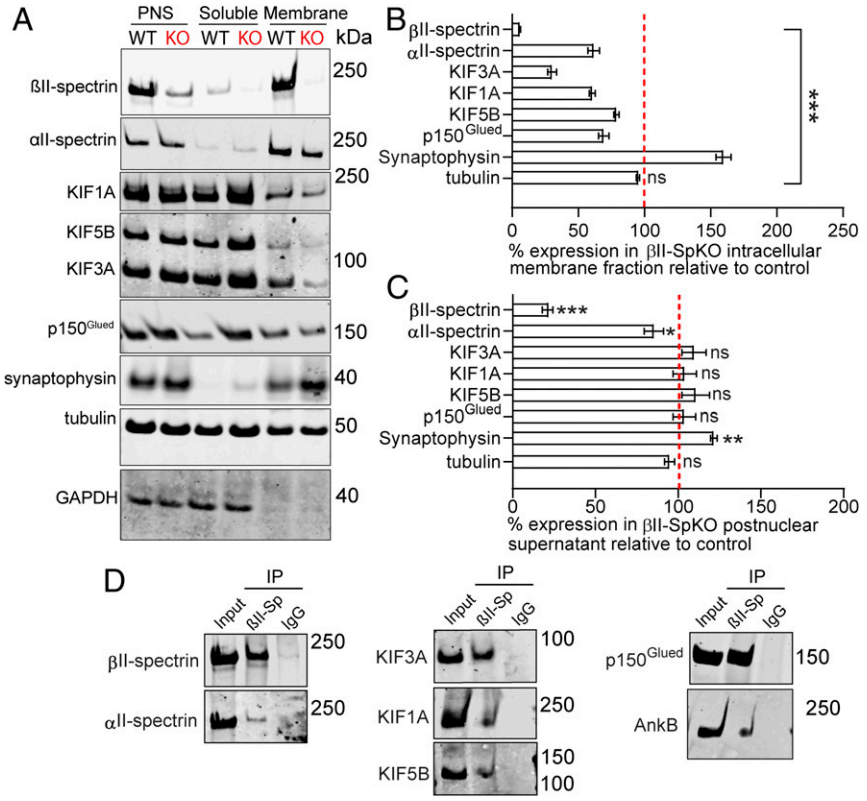

Fig. 6. βII-spectrin forms protein complexes with motor proteins and is required for their association with intracellular membranes. (*A–C*) Immunoblots (*A*) and corresponding quantification of protein levels of βII-spectrin, αII-spectrin, dynactin (p150^{Glued}), KIF1A, KIF3A, KIF5B, and synaptophysin in intracellular membrane (*B*) and postnuclear supernatant fractions (*C*) evaluated after subcellular fractionation of brain homogenates. Synaptophysin is a fractionation control. Tubulin and GAPDH are loading controls. Data represent mean ± SEM. One-way ANOVA with Dunnett's multiple comparisons test, ***$P < 0.001$, **$P < 0.01$, *$P < 0.05$. ns, not significant. (*D*) Western blot of the input and elution fraction from brain homogenates immunoprecipitated with a rabbit βII-spectrin antibody or isotype IgG control and immunoblotted with antibodies specific for βII-spectrin, αII-spectrin, AnkB, p150^{Glued}, KIF1A, KIF3A, and KIF1A.

H). As observed in older neurons, synaptic vesicle dynamics in DIV2 βII-spectrin KO were deficient relative to control neurons, but like in control neurons, organelle dynamics were similar between the proximal and the distal axon regions (Fig. 7 *D, G*, and *H*). These observations suggest that assembly of the periodic actin–spectrin skeleton is not required to enable the intracellular transport machinery. Thus, βII-spectrin independently assembles the neuronal actin periodic structure and promotes axonal organelle transport.

βII-Spectrin and AnkB Independently Enable Axonal Organelle Transport. The axonal transport and growth deficits of βII-SpKO neurons and the loss of long-range axonal connectivity in βII-SpKO mouse brains resemble phenotypes observed upon loss of AnkB (14, 40); 220-kDa AnkB promotes axonal organelle transport via dual interactions with PI3P phosphoinositide lipids on membranes and the p62/dynactin4 subunit of the dynein/dynactin motor complex (14). Therefore, we asked whether βII-spectrin requires AnkB binding to promote axonal transport and growth. To our surprise, we found that mScarlet-tagged Y1874A βII-spectrin, which is unable to bind AnkB (Fig. 3*D*) (41), rescued both synaptic vesicle transport (Fig. 5 *A–E*) and axonal length (Fig. 3 *B* and *C*) deficits in neurons lacking βII-spectrin. The strong effects of loss of βII-spectrin on anterograde cargo motion, which are not observed in AnkB-deficient neurons, together with results from our rescue experiments, suggest that βII-spectrin promotes axonal transport independently of AnkB.

Previous studies using reconstituted motility assays using squid axon's cytoplasmic material and liposomes coated with acidic phospholipids showed that a dominant-negative construct containing the pleckstrin homology (PH) domain of βII-spectrin affected organelle and liposome retrograde motility, suggesting that β-spectrin's association with membrane lipids is required for dynein/dynactin-driven axonal transport (42). The βII-spectrin PH domain interacts with PI(4,5)P, PI(3,4)P2, and PI(3,4,5)P3 lipids through a highly conserved binding pocket (43). Mutation of a basic PH domain residue (K2207Q) (Fig. 3*D*) eliminated binding of *Drosophila* β-spectrin as well as mammalian βII-spectrin to these phosphoinositides (41, 44). Thus, we next evaluated synaptophysin–YFP dynamics in βII-SpKO neurons transfected with mScarlet-tagged K2207Q βII-spectrin and found that this mutant failed to restore both axonal transport (Fig. 5 *A–E*) and axon length (Fig. 3 *B* and *C*). These data indicate that βII-spectrin binding to PIP lipids is required for its functions in axonal transport and growth.

Finally, we employed a genetic approach to determine whether βII-spectrin and AnkB promote axonal transport through independent pathways. If this were the case, dual loss of these proteins would cause a more severe impairment of transport dynamics than their individual deficits. To test this prediction, we developed mice bearing homozygous copies of both βII-spectrin and AnkB floxed alleles (*AnkB$^{flox/flox}$*; *βII-Spec$^{flox/flox}$*) and crossed them to Nestin-Cre to eliminate both proteins in all neuronal precursors. While individual KO of either AnkB or βII-spectrin in the brains causes postnatal lethality, their combined loss results in early embryonic death, with no *AnkB$^{flox/flox}$;βII-Spec$^{flox/flox}$*;Nestin-Cre/+ animals recovered. However, mice with total loss of one of these two genes and 50% reduction in the other (*AnkB$^{flox/flox}$;βII-Spec$^{flox/+}$*;Nestin-Cre/+ or *AnkB$^{flox/+}$;βII-Spec$^{flox/flox}$*;Nestin-Cre/+) showed earlier lethality and more severe morphological deficits and motor impairments than either each of the single gene KO or the double-heterozygous mice (Fig. 8 *A* and *B*). To overcome the embryonic lethality associated with double KO of neuronal AnkB and βII-spectrin, we cultured hippocampal neurons from embryonic *AnkB$^{flox/flox}$;βII-Spec$^{flox/flox}$* animals and cotransfected them at plating (DIV0) with synaptophysin–YFP to assess synaptic vesicles dynamics, and with either control pBFP or pBFP-Cre plasmids. Kymograph analysis from time-lapse movies of synaptophysin–YFP in axons reveal a dramatic reduction in motile synaptic cargo (red and green lines) in Cre-BFP–expressing *AnkB$^{flox/flox}$;βII-Spec$^{flox/flox}$* axons (Fig. 8 *C, F*, and *G*). Simultaneous loss of AnkB and βII-spectrin in neurons almost entirely stalled synaptic vesicle transport. The few synaptophysin–YFP-positive vesicles that retained motility exhibited further reductions in both anterograde and retrograde

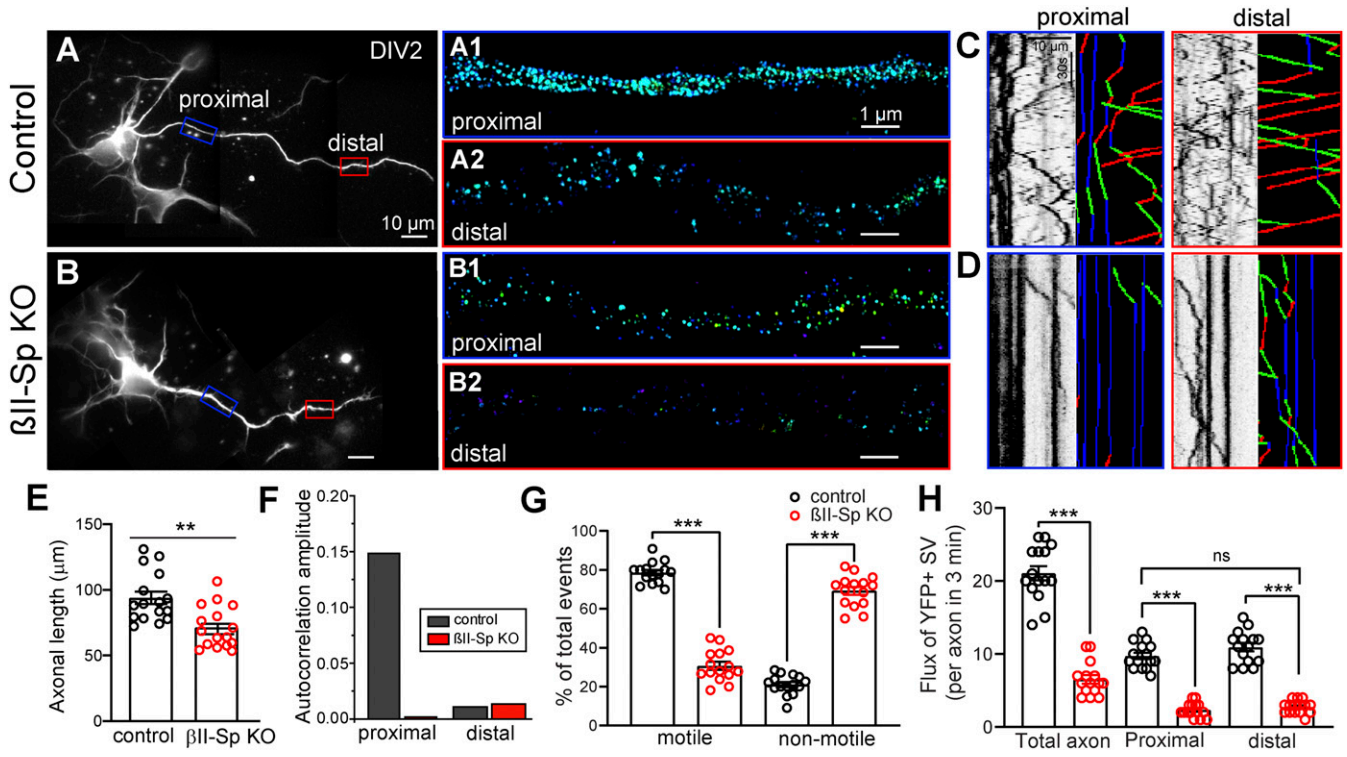

Fig. 7. Axonal transport deficits in βII-spectrin KO neurons appear early in axonal development. Normal axonal transport precedes the assembly of the actin–spectrin periodic skeleton. (*A* and *B*) DIV2 control (*A*) and βII-SpKO (*B*) cortical neurons labeled with β-tubulin. Rectangles demark proximal (blue) and distal (red) regions of the axon. (Scale bars, 10 μm.) Three-dimensional STORM images of βII-spectrin in the proximal (control, *A1* and βII-SpKO, *B1*) and the distal (control, *A2* and βII-SpKO, *B2*) axonal regions of DIV2 cortical neurons. (Scale bars, 1 μm.) (*C* and *D*) Kymographs showing the mobility of YFP-tagged synaptophysin-positive synaptic vesicles in the proximal (blue outlines) and distal (red outlines) axon regions in control (*C*) and βII-SpKO (*D*) cortical neurons. Trajectories are shown in green for anterograde, red for retrograde, and blue for static vesicles. (Scale bar, 10 μm and 30 s.) (*E*) Axonal length in control ($n = 16$) and βII-SpKO ($n = 16$) DIV2 cortical neurons. (*F*) Average autocorrelation amplitude of βII-spectrin calculated from multiple, randomly selected cortical neurons. Axon proximal ($n = 23$) and distal ($n = 40$) regions for $\beta IISp^{flox/flox}$/+ samples. Axon proximal ($n = 39$) and distal ($n = 37$) regions for $\beta IISp^{flox/flox}$/Nestin-Cre samples. (*G*) Relative number of motile synaptic vesicles in DIV2 $\beta IISp^{flox/flox}$/+ ($n = 21$) and $\beta IISp^{flox/flox}$/Nestin-Cre (KO) ($n = 23$) axons. (*H*) Quantification of flux of synaptic vesicles along the total length, the proximal, and the distal regions of the axons of in DIV2 $\beta IISp^{flox/flox}$/+ ($n = 21$), $\beta IISp^{flox/flox}$/Nestin-Cre (KO) ($n = 23$) cortical neurons. Data represent mean ± SEM. Student's *t* test, $***P < 0.001$, $**P < 0.01$. ns, not significant.

velocity and run length parameters (Fig. 8 *D* and *E*). That dual loss of these transport facilitators causes a more severe impairment of transport dynamics than their individual deficits supports the conclusion that AnkB and βII-spectrin promote axonal transport of synaptic cargo through independent pathways.

Discussion

In this study we present direct in vivo evidence that βII-spectrin multitasks in mouse brain, with important roles in both establishing the membrane-associated periodic skeleton as well as enabling axonal transport of synaptic cargo. These biochemical activities, although involving distinct molecular partners and cellular locations, have a concerted effect in promoting both axon growth and stability. Our finding that βII-spectrin promotes axonal transport was foreshadowed by the identification of β-spectrin polypeptides comigrating with axonal cargo in the optic nerve nearly 40 y ago (11), and more recently by observations that α-II spectrin associates with and comigrates with kinesin (12), that spectrin is required to reconstitute dynactin-dependent motility of liposomes (42), and that introduction of human SCA5 mutations into *Drosophila* β-spectrin impairs axonal organelle transport (13). Interestingly, AnkB, which is a βII-spectrin partner in vitro and in vivo (18, 45, 46), also promotes axonal organelle transport and is required for formation of long axon tracts in the developing brain (14). However, we find that βII-spectrin and AnkB promote axonal transport through distinct mechanisms. βII-spectrin lacking ankyrin-binding activity restores transport, while mice lacking both βII-spectrin and AnkB exhibit more severely impaired axonal transport than those missing either protein alone. Instead of utilizing AnkB to associate with organelle membranes, βII-spectrin likely connects through interaction with PIP lipids, since mutation of its PH domain eliminating binding to PI(3,4)P2, PI(4,5)P2, and PI(3,4,5)P3 also prevents rescue of axonal transport and axon length. Strikingly, neurons lacking both βII-spectrin and AnkB exhibit a nearly complete loss of both anterograde and retrograde axonal transport of synaptic cargo, and brain-specific, double βII-spectrin and AnkB KO mice die embryonically.

The finding that axonal transport of synaptic cargo is nearly eliminated by dual loss of βII-spectrin and AnkB was unexpected, given the diversity of kinesins, kinesin binding-proteins, and partners for dynein/dynactin (47, 48). We, therefore, experimentally evaluated alternatives to roles of these proteins as transport facilitators whereby they enable the coupling of organelles to motors. For example, βII-spectrin and the periodic actin rings have been proposed to be required for microtubule stability (36). However, deficiency of βII-spectrin (*SI Appendix*, Fig. S8 *A–D*) or AnkB (14) had no effect on microtubule dynamics or polarity by direct imaging of EB3-tdT–labled microtubule fast-growing ends. Additionally, as we showed, organelle transport proceeds normally through regions in the axon before the actin–spectrin periodic structure forms. Thus, we propose that βII-spectrin and AnkB are versatile motor cofactors that promote the long-range axonal transport of multiple organelles. The orchestration of the tethering and precise delivery of cargo along the axon are not fully understood. The prevailing view consists of a model where multiple activators, adaptors, and

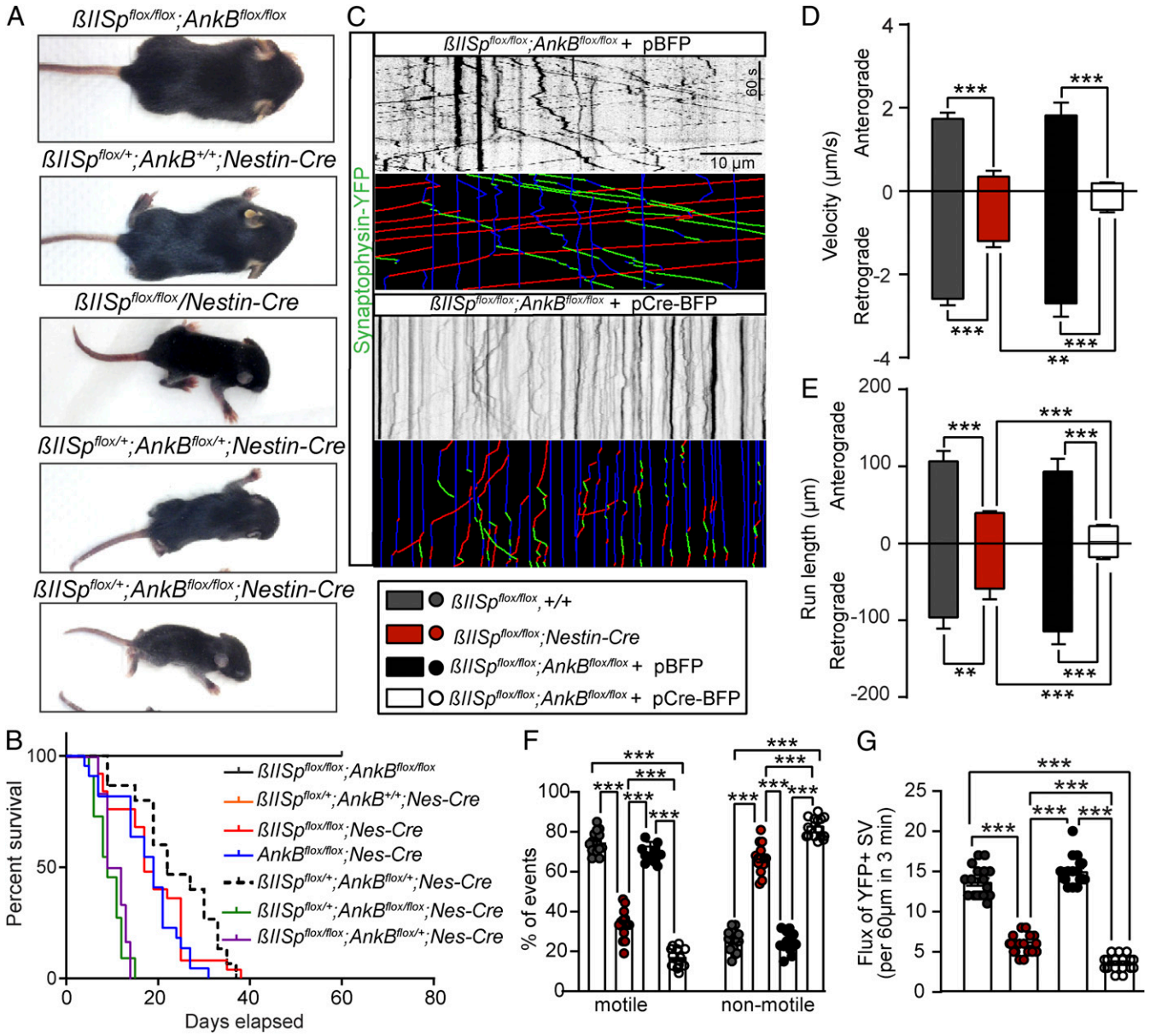

Fig. 8. Independent βII-spectrin and AnkB pathways promote axonal transport. (*A*) PND8 mice of the indicated genotypes. (*B*) Mice survival curves. A Mantel–Cox test was used to compare survival. (*C*) Kymographs showing the mobility of YFP-tagged synaptophysin-positive synaptic vesicles in axons from $\beta IISp^{flox/flox};AnkB^{flox/flox}$ neurons transfected with either pBFP or pCre-BFP plasmids. Trajectories are shown in green for anterograde, red for retrograde, and blue for static vesicles. (Scale bar, 10 µm and 60 s.) (*D*–*G*) Anterograde and retrograde velocity (*D*), run length (*E*), relative number of motile and nonmotile synaptic vesicles (*F*), and quantification of flux (*G*) of synaptic vesicles in $\beta IISp^{flox/flox}$ (anterograde $n = 76$, retrograde $n = 94$), $\beta IISp^{flox/flox}$/Nestin-Cre (anterograde $n = 55$, retrograde $n = 68$) axons, and in axons of $\beta IISp^{flox/flox};AnkB^{flox/flox}$ neurons transfected with BFP (anterograde $n = 75$, retrograde $n = 91$) or Cre-BFP (anterograde $n = 127$, retrograde $n = 119$) of DIV7 neurons. Data represent mean ± SEM. One-way ANOVA with Dunnett's multiple comparisons test, $^{***}P < 0.001$, $^{**}P < 0.01$.

cofactors facilitate the processivity and selective coupling of motors to specific membrane cargos (47, 49, 50). Our current data support βII-spectrin and AnkB as principal motor cofactors for at least synaptic cargo in axons. Going forward it will be critical to elucidate the full scope of organelles that depend on βII-spectrin for axonal transport and determine at a molecular level how βII-spectrin interacts with motor complexes.

Recent cryo-EM structures of dynactin propose that its $p150^{Glued}$ subunit is sterically less hindered than the Arp1 subunit (47). While Arp1 has been shown to interact with spectrin in vitro and under conditions of overexpression (18), the cryo-EM data support our results suggesting that βII-spectrin may also bind $p150^{Glued}$. Similarly, it is not clear whether βII-spectrin interacts with KIF3A, KIF5B, KIF1A, and perhaps other kinesins, directly or through intermediary protein(s). Finally, it will be of interest to determine the roles of β-spectrins and AnkB in cellular domains in addition to axons, which are highly specialized for long-range transport. β-spectrin homologs are not evident in genomes of fungi or plants. Kinesins and dynein/dynactin thus were present nearly a billion years before spectrins. Therefore, interactions of spectrins with motor proteins evolved in the context of multicellularity, and likely will turn out to include features that are cell type- and/or cell domain-specific.

Materials and Methods

Detailed materials and methods, including statistical analysis, are described in *SI Appendix, Materials and Methods*. Experiments were performed in accordance with the guidelines for animal care of the institutional animal care

and use committee at Duke University and the University of North Carolina at Chapel Hill. All mice were housed at 22 °C ± 2 °C on a 12-h-light/12-h-dark cycle and fed regular chow and water for ad libitum consumption. For full details about the generation of the mice used in these studies and the EM, STORM, DTI, and intracellular transport experiments see *SI Appendix, Materials and Methods*.

ACKNOWLEDGMENTS. We thank Dr. Matthew Rasband for the gift of the βII-spectrin conditional KO mice; Erica Robinson, Janell Hostettler, Liset Falcón, and Christopher Gabriel for experimental assistance; Dr. Evan Heller for help with STORM imaging of actin and adducin in neurons; and the Duke Center for In Vivo Microscopy (CIVM) staff, in particular Yi Qi for mouse perfusion and George A. Johnson, Natalie Delpratt, and Robert J. Anderson for DTI data analysis and consultation. D.N.L. was supported by the University of North Carolina at Chapel Hill School of Medicine as a Simmons Scholar, by the National Ataxia Foundation, and by the Howard Hughes Medical Institute (HHMI). R.Z. and X.Z. were supported by the NIH (R35GM122487) and the HHMI. P.J.M. was supported by the NIH (R35HL135754). V.B. was supported by the HHMI and a George Barth Geller endowed professorship. DTI imaging was funded by a Kahn Neurotechnology Development grant to A.B. and V.B. and K01 AG041211 to A.B. CIVM is supported in part by P41 EB015897. Work using the Microscopy Core was also supported by Grant P30 NS045892 to the University of North Carolina Neuroscience Center.

1. V. Bennett, D. N. Lorenzo, Spectrin- and ankyrin-based membrane domains and the evolution of vertebrates. *Curr. Top. Membr.* **72**, 1–37 (2013).
2. V. Bennett, D. N. Lorenzo, An adaptable spectrin/ankyrin-based mechanism for long-range organization of plasma membranes in vertebrate tissues. *Curr. Top. Membr.* **77**, 143–184 (2016).
3. T. J. Byers, D. Branton, Visualization of the protein associations in the erythrocyte membrane skeleton. *Proc. Natl. Acad. Sci. U.S.A.* **82**, 6153–6157 (1985).
4. K. Xu, G. Zhong, X. Zhuang, Actin, spectrin, and associated proteins form a periodic cytoskeletal structure in axons. *Science* **339**, 452–456 (2013).
5. Y. M. Sigal, R. Zhou, X. Zhuang, Visualizing and discovering cellular structures with super-resolution microscopy. *Science* **361**, 880–887 (2018).
6. D. S. Gokhin, V. M. Fowler, Feisty filaments: Actin dynamics in the red blood cell membrane skeleton. *Curr. Opin. Hematol.* **23**, 206–214 (2016).
7. B. Han, R. Zhou, C. Xia, X. Zhuang, Structural organization of the actin-spectrin-based membrane skeleton in dendrites and soma of neurons. *Proc. Natl. Acad. Sci. U.S.A.* **114**, E6678–E6685 (2017).
8. P. Agre, E. P. Orringer, V. Bennett, Deficient red-cell spectrin in severe, recessively inherited spherocytosis. *N. Engl. J. Med.* **306**, 1155–1161 (1982).
9. M. Hammarlund, E. M. Jorgensen, M. J. Bastiani, Axons break in animals lacking beta-spectrin. *J. Cell Biol.* **176**, 269–275 (2007).
10. N. Chakrabarty *et al.*, Processive flow by biased polymerization mediates the slow axonal transport of actin. *J. Cell Biol.* **218**, 112–124 (2019).
11. R. Cheney, N. Hirokawa, J. Levine, M. Willard, Intracellular movement of fodrin. *Cell Motil.* **3**, 649–655 (1983).
12. S. Takeda *et al.*, Kinesin superfamily protein 3 (KIF3) motor transports fodrin-associating vesicles important for neurite building. *J. Cell Biol.* **148**, 1255–1265 (2000).
13. D. N. Lorenzo *et al.*, Spectrin mutations that cause spinocerebellar ataxia type 5 impair axonal transport and induce neurodegeneration in Drosophila. *J. Cell Biol.* **189**, 143–158 (2010).
14. D. N. Lorenzo *et al.*, A PIK3C3-ankyrin-B-dynactin pathway promotes axonal growth and multiorganelle transport. *J. Cell Biol.* **207**, 735–752 (2014).
15. F. Qu *et al.*, Ankyrin-B is a PI3P effector that promotes polarized α5β1-integrin recycling via recruiting RabGAP1L to early endosomes. *eLife* **5**, e20417 (2016).
16. N. Hirokawa, S. Niwa, Y. Tanaka, Molecular motors in neurons: Transport mechanisms and roles in brain function, development, and disease. *Neuron* **68**, 610–638 (2010).
17. J. Davis, V. Bennett, Brain spectrin. Isolation of subunits and formation of hybrids with erythrocyte spectrin subunits. *J. Biol. Chem.* **258**, 7757–7766 (1983).
18. E. A. Holleran, M. K. Tokito, S. Karki, E. L. Holzbaur, Centractin (ARP1) associates with spectrin revealing a potential mechanism to link dynactin to intracellular organelles. *J. Cell Biol.* **135**, 1815–1829 (1996).
19. G. Ayalon, J. Q. Davis, P. B. Scotland, V. Bennett, An ankyrin-based mechanism for functional organization of dystrophin and dystroglycan. *Cell* **135**, 1189–1200 (2008).
20. M. He, W. C. Tseng, V. Bennett, A single divergent exon inhibits ankyrin-B association with the plasma membrane. *J. Biol. Chem.* **288**, 14769–14779 (2013).
21. M. C. Stankewich *et al.*, Targeted deletion of betaIII spectrin impairs synaptogenesis and generates ataxic and seizure phenotypes. *Proc. Natl. Acad. Sci. U.S.A.* **107**, 6022–6027 (2010).
22. S. Berghs *et al.*, betaIV spectrin, a new spectrin localized at axon initial segments and nodes of ranvier in the central and peripheral nervous system. *J. Cell Biol.* **151**, 985–1002 (2000).
23. D. M. Bodine , 4th, C. S. Birkenmeier, J. E. Barker, Spectrin deficient inherited hemolytic anemias in the mouse: Characterization by spectrin synthesis and mRNA activity in reticulocytes. *Cell* **37**, 721–729 (1984).
24. Y. Ikeda *et al.*, Spectrin mutations cause spinocerebellar ataxia type 5. *Nat. Genet.* **38**, 184–190 (2006).
25. C. C. Wang *et al.*, βIV spectrinopathies cause profound intellectual disability, congenital hypotonia, and motor axonal neuropathy. *Am. J. Hum. Genet.* **102**, 1158–1168 (2018).
26. Y. Tang *et al.*, Disruption of transforming growth factor-beta signaling in ELF beta-spectrin-deficient mice. *Science* **299**, 574–577 (2003).
27. M. R. Galiano *et al.*, A distal axonal cytoskeleton forms an intra-axonal boundary that controls axon initial segment assembly. *Cell* **149**, 1125–1139 (2012).
28. Y. Uemoto *et al.*, Specific role of the truncated betaIV-spectrin Sigma6 in sodium channel clustering at axon initial segments and nodes of ranvier. *J. Biol. Chem.* **282**, 6548–6555 (2007).
29. S. Lambert, V. Bennett, Postmitotic expression of ankyrinR and beta R-spectrin in discrete neuronal populations of the rat brain. *J. Neurosci.* **13**, 3725–3735 (1993).
30. Y. L. Clarkson *et al.*, β-III spectrin underpins ankyrin R function in Purkinje cell dendritic trees: Protein complex critical for sodium channel activity is impaired by SCA5-associated mutations. *Hum. Mol. Genet.* **23**, 3875–3882 (2014).
31. E. Calabrese, A. Badea, G. Cofer, Y. Qi, G. A. Johnson, A diffusion MRI tractography connectome of the mouse brain and comparison with neuronal tracer data. *Cereb. Cortex* **25**, 4628–4637 (2015).
32. C. Y. Huang, C. Zhang, D. R. Zollinger, C. Leterrier, M. N. Rasband, An αII spectrin-based cytoskeleton protects large-diameter myelinated axons from degeneration. *J. Neurosci.* **37**, 11323–11334 (2017).
33. S. C. Leite *et al.*, The actin-binding protein α-adducin is required for maintaining axon diameter. *Cell Rep.* **15**, 490–498 (2016).
34. M. J. Rust, M. Bates, X. Zhuang, Sub-diffraction-limit imaging by stochastic optical reconstruction microscopy (STORM). *Nat. Methods* **3**, 793–795 (2006).
35. B. Huang, W. Wang, M. Bates, X. Zhuang, Three-dimensional super-resolution imaging by stochastic optical reconstruction microscopy. *Science* **319**, 810–813 (2008).
36. Y. Qu, I. Hahn, S. E. D. Webb, S. P. Pearce, A. Prokop, Periodic actin structures in neuronal axons are required to maintain microtubules. *Mol. Biol. Cell* **28**, 296–308 (2017).
37. P. J. Hollenbeck, D. Bray, Rapidly transported organelles containing membrane and cytoskeletal components: Their relation to axonal growth. *J. Cell Biol.* **105**, 2827–2835 (1987).
38. K. J. De Vos, M. Hafezparast, Neurobiology of axonal transport defects in motor neuron diseases: Opportunities for translational research? *Neurobiol. Dis.* **105**, 283–299 (2017).
39. G. Zhong *et al.*, Developmental mechanism of the periodic membrane skeleton in axons. *eLife* **3**, e04581 (2014).
40. P. Scotland, D. Zhou, H. Benveniste, V. Bennett, Nervous system defects of AnkyrinB (-/-) mice suggest functional overlap between the cell adhesion molecule L1 and 440-kD AnkyrinB in premyelinated axons. *J. Cell Biol.* **143**, 1305–1315 (1998).
41. M. He, K. M. Abdi, V. Bennett, Ankyrin-G palmitoylation and βII-spectrin binding to phosphoinositide lipids drive lateral membrane assembly. *J. Cell Biol.* **206**, 273–288 (2014).
42. V. Muresan *et al.*, Dynactin-dependent, dynein-driven vesicle transport in the absence of membrane proteins: A role for spectrin and acidic phospholipids. *Mol. Cell* **7**, 173–183 (2001).
43. M. Hyvönen *et al.*, Structure of the binding site for inositol phosphates in a PH domain. *EMBO J.* **14**, 4676–4685 (1995).
44. A. Das, C. Base, D. Manna, W. Cho, R. R. Dubreuil, Unexpected complexity in the mechanisms that target assembly of the spectrin cytoskeleton. *J. Biol. Chem.* **283**, 12643–12653 (2008).
45. P. Agre, J. F. Casella, W. H. Zinkham, C. McMillan, V. Bennett, Partial deficiency of erythrocyte spectrin in hereditary spherocytosis. *Nature* **314**, 380–383 (1985).
46. P. J. Mohler, W. Yoon, V. Bennett, Ankyrin-B targets beta2-spectrin to an intracellular compartment in neonatal cardiomyocytes. *J. Biol. Chem.* **279**, 40185–40193 (2004).
47. S. L. Reck-Peterson, W. B. Redwine, R. D. Vale, A. P. Carter, The cytoplasmic dynein transport machinery and its many cargoes. *Nat. Rev. Mol. Cell Biol.* **19**, 382–398 (2018).
48. N. Hirokawa, Y. Noda, Intracellular transport and kinesin superfamily proteins, KIFs: Structure, function, and dynamics. *Physiol. Rev.* **88**, 1089–1118 (2008).
49. A. Akhmanova, J. A. Hammer , 3rd, Linking molecular motors to membrane cargo. *Curr. Opin. Cell Biol.* **22**, 479–487 (2010).
50. S. Maday, A. E. Twelvetrees, A. J. Moughamian, E. L. F. Holzbaur, Axonal transport: Cargo-specific mechanisms of motility and regulation. *Neuron* **84**, 292–309 (2014).